INTERACTION OF METRONIDAZOLE WITH ALDEHYDE DEHYDROGENASE: SPECTROSCOPIC APPROACH

OLURANTI ESTHER OLAIYA, ADEJOKE NAOMI KOLAWOLE, AO. KOLAWOLE[#]

Biomolecular Structure and Dynamics Unit, Department of Biochemistry, The Federal University of Technology, Akure, Nigeria, [#]e-mail: aokolawole@futa.edu.ng

Abstract. The interaction between metronidazole and some vital proteins, which exaggerates the reported toxicity of the drug, is uncertain. Herein, the molecular interaction between aldehyde dehydrogenase (ALDH), a major detoxifying enzyme with pathophysiological implications, and metronidazole was investigated by spectroscopy techniques. Spectrofluorimetric measurements revealed that metronidazole quenched the ALDH intrinsic fluorescence through a non-fluorescent ALDH-metronidazole complex. Dynamic quenching and non-radiative energy transfer were responsible for the bathochromic fluorescence quenching. Thermodynamic analysis showed that metronidazole binds to ALDH via hydrogen and van der Waals interactions. The association was not spontaneous but enough to cause perturbation of the protein structure. The enzyme has approximately two association sites for metronidazole, non-cooperative binding, with a binding constant (K_a) of 5.8×10^3 $L\cdot M^{-1}$. The association of the complex was favorable compared to its dissociation at temperatures and pH studied. The fluorescence emission quenching obeys FRET phenomenon with a R = 3.42 nm. ALDH as nano-particles in a drug delivery of metronidazole for detoxification is hereby suggested.

Key words: Aldehyde dehydrogenases, fluorescence quenching metronidazole, spectroscopy.

INTRODUCTION

Aldehyde dehydrogenases (ALDH; EC 1.2.1.3), short-chain dehydrogenases/reductases (SDR), are polymorphic superfamily of multifunctional NAD(P)+ dependent enzyme that catalyses the oxidation (dehydrogenation) of aldehydes to their corresponding carboxylic acid [16, 18, 23]. ALDH group of isoenzyme have multifaceted physiological and toxicologically roles and are involved in cellular response to oxidative stress and detoxification of stress generated aldehydes [16]. Aldehydes are cytotoxic and mutagenic. ALDHs modulate cell proliferation, differentiation and survival and support cellular homeostasis [23]. The metabolic and regulatory properties of ALDH isoenzymes are connected cancerous cell related diseases, myocardial ischemia, Alzheimer's

Received March 2017;
in final form April 2007.

ROMANIAN J. BIOPHYS., Vol. 26, No. 4, P. 000–000, BUCHAREST, 2016

and Parkinson's diseases, Sjorgren-Larsson syndrome and alcohols-related pathology [4, 10, 15, 16, 18, 19,]. LDH catalytic mechanism has been investigated extensively [27, 43] and is reported to be sequential mechanism. ALDHs, however, have several non-enzymatic functions such as binding to some hormones and other small molecules [23, 35]. This clearly referred to its non-catalytic binding properties for small and structurally diverse endobiotics and xenobiotics [1, 12]. This function has been implicated in the ALDH detoxification by sequestration of accumulation of small molecules in the cells when the concentration becomes overwhelming. Little is known about this ligand binding functions.

Metronidazole [1-(2-hydroxyethyl)-2-methyl-5-nitroimidazole], a nitroimidazole compound is a commonly used antibiotic, effective in treating anaerobic bacterial and protozoan infections [31]. The molecular structure is shown in Fig. 1. It has been used for the treatment of trichomoniasis [1] and inflammatory bowel disease [2]. Metronidazole has immunosuppressive properties and is a drug of choice for treatment of Crohn's disease [32]. It is one of the groups of clinically significant heterocyclic radio sensitizing drugs [22]. Therapeutic impact of metronidazole runs with high rate of side effects. Metronidazole is mutagenic for bacteria and carcinogenic in mice. Metronidazole related has a documented harmful effect on human [50], nitroimidazoles have been banned from use in food producing animals within the European Union, the US and other countries including China. There is no report of the drug being banned in Nigeria and other West African countries. It has become one of the over counter drugs [49]. However, the potential toxic effects of metronidazole to detoxification related enzymes seem not to have attract attention in metronidazole toxicity, lately. To fill the gap, we investigated the toxicity of metronidazole to ALDH in this study using spectroscopic approach.

Various spectroscopic methods such as absorption, fluorescence, circular dichroism (CD), nuclear magnetic resonance (NMR), and electron spin resonance (ESR), have been adopted in the past for measuring the binding constants of small molecules with large macromolecules [28]. Fluorescence spectrometry is an effective, and very accessible tool to thermodynamically characterized ligand-protein binding phenomenon [11, 13, 48]. It essentially probes changes in the local microenvironment of the fluorophore (fluorescent chromophore), which has been widely used for drug-protein studies and provide clue to the nature of the binding characteristics. The method is high sensitive, accurate, rapid, convenient and simple [37, 41].

Current hypothetical reasoning suggests that factors such as other protein binding may impair drugs absorption and bioavailability and even mask their therapeutics or its toxicity and side effects. However, little attention has been directed to interactions of the important and abused compounds with the other detoxifying and ligand binding enzymes. These are in a strategic position to limit

the efficacy of the drug and exaggerate the side effects and toxicity. With these, thermodynamic basis, affinity and binding parameters of non-substrate ligand binding of ALDH to metronidazole were sought. This should be of great importance of toxicology/detoxification point of view.

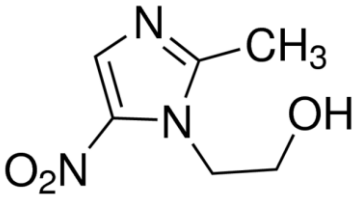

Fig. 1. Structure of metronidazole.

MATERIALS AND METHODS

MATERIALS

Baker's yeast aldehyde dehydrogenase (ALDH) molecular weight 200,000 Dalton (Millipore EMD Millipore Corporation, Billerica, MA, USA) was used without further purification. Trizma base, potassium phosphate monobasic, di-potassium hydrogen phosphate, acetic acid, sodium acetate, hydrochloric acid, were purchased from Sigma-Aldrich Fine Chemicals (St. Louis, MO, USA). Bovine Serum Albumin standard and Bradford reagent were products of BioRad (Palo Alto, CA, USA). Pure Metronidazole (Pharmaceutical grade, > 99%) was a generous gift from Sam Pharmaceutical limited (Ilorin, Nigeria). All other chemicals were commercial products of analytical reagent grade and used without any purification. The stock solution of metronidazole (molecular weight of 171.15g/mol) was prepared in double distilled absolute ethanol. Reagents solutions and buffers used were filtered with a Millipore membrane filter (0.45 micron filter, VWR, USA) immediately before use. ALDH protein concentrations were measured by Bradford method. pH was monitored by Crison pH meter BASIC 20^{+} (Crison Instruments, Barcelona, Spain)

FLUORESCENCE MEASUREMENTS

Hitachi F-4500 fluorescence spectrometer (Hitachi Ltd., Tokyo, Japan) interfaced to a refrigerated circulating water bath (Pharmacia Biotech, Uppsala, Sweden) and 1.0 cm quartz cell was used to obtain the fluorescence emission spectra and synchronous spectra. Fluorescence emission data were stored at 10 Hz sampling rate to a Dell PC (Windows XP). The spectra were recorded in the

wavelength range of 300–500 nm upon excitation at 280 nm when ALDH samples were titrated with metronidazole. Both excitation and emission bandwidths were set at 5 nm with a scan speed of 900 nm/min and a response time of 2 s. Titrations were performed manually by using trace syringes. A 2.0 mL solution containing an appropriate concentration of ALDH (0.250 μM) in 25 mM Tris-HCl at pH = 7.4 containing 0.1 M NaCl was titrated manually by successive additions of ethanol stock solution of metronidazole to final concentrations of 100 μM. The presence of this volume of ethanol in the assay mixtures had no effect on the fluorescence measurements. Also, respective blanks of the buffer were used for the correction of all fluorescence spectra. The experiments were conveniently reproducible. The maximum emission intensities were used to calculate the binding constants, the number of binding sites and thermodynamic parameters. Synchronous fluorescence spectroscopy (SFS) was used to study the environment of amino acid residues. It involves the measurement of any shift of the emission maximum, to reflect the changes of polarity around the chromophore molecule, on addition of ligand molecules. Synchronous fluorescence spectra of solutions prepared as above were measured on the same fluorescence spectrometer. The excitation wavelength (λ_{ex}) was set at 280 nm. The excitation and emission slit widths were set at 5.0 nm. The D-value ($\Delta\lambda$) between the excitation and emission wavelengths was set at 15 or 60 nm. PMT voltage was 700V.

UV-VISIBLE ABSORPTION SPECTROSCOPY

UV-1800 Shimadzu double beam UV-Visible spectrophotometer (Shimadzu Corporation, Tokyo, Japan) equipped with a Pharmacia refrigerating circulator for temperature control was used to record UV-Vis spectra. The scan speed and slit of absorbance (λ_{abs}) were set to medium and 1.0 nm respectively. The spectra were recorded between 200–500 nm. A 1.0 mL solution of 0.250 μM ALDH was titrated with successive addition of metronidazole. Each result was the average of the three scans.

STATISTICAL ANALYSIS

Graphical analysis for ALDH-metronidazole adduct were performed using KaleidaGraph 4.5 software (Synergy software, Reading, PA, USA) for Macintosh Computer.

RESULTS AND DISCUSSION

CHARACTERISTICS OF ALDH-METRONIDAZOLE FLUORESCENCE SPECTRA

The fluorescence spectroscopy was used to determine the nature of interaction between metronidazole and ALDH. The fluorescence spectra of ALDH with different concentrations of metronidazole are shown in Fig. 2. The maximum of fluorescence emission of the protein in the absence of the ligand (metronidazole) was at 350 nm, after excitation at 280 nm. The intensity and position of fluorescence maximum are related to microenvironment of the tryptophan and tyrosine residues in ALDH [6]. Metronidazole was non-fluorescent and the possible inner filter effect was corrected as described elsewhere [39]. The fluorescence intensities of ALDH decreased gradually with the concentration of metronidazole (0–110 μM). This indicates strong binding of metronidazole with ALDH. Fluorescence quenching refers to any process which decreases the fluorescence intensity of certain fluorophores with phenomenological and application instincts, most often, in protein-ligand interaction studies [33]. The fluorescence quenching can result from a variety of molecular interactions – molecular rearrangement of ground state complex formations, excited-state reactions, energy transfer and collision quenching [25].

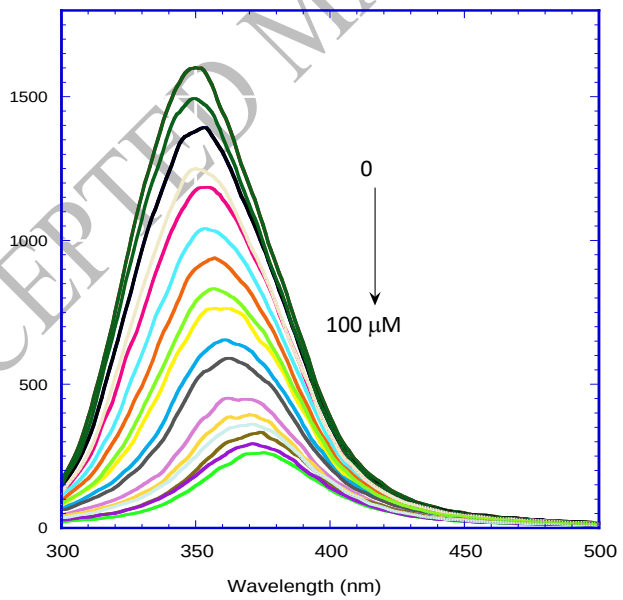

Fig. 2. Effect of metronidazole (0–110 μM) on the intrinsic fluorescence of ALDH 0.25 μM) at 25 °C and pH 7.4. The excitation wavelength was 280 nm and the spectra were recorded between 300–500 nm.

These interactions cause changes in the fluorescence spectra. There was a significant bathochromic shift of 25 nm, from 350 nm to 375 nm. The red shift result was not unusual. This observation was in agreement with earlier observations of the interaction of metronidazole with bovine serum albumin [18, 43]. This is connected to exposure of fluorophores to a more hydrophilic environment. The tendency of metronidazole to hydrate the hydrophobic core of protein might be connected to its small phenolic structure and its probing functional groups. The interaction makes it less hydrophobic making the Met-ALDH complex less compact. This could lead to a large enthalpic penalty.

The mechanism of fluorescence quenching can be either dynamic or static and in some cases both. The dynamic quenching mechanism is dependent of diffusion while the static quenching mechanism is not [9]. The quenching rate constants decrease with increasing temperature for static quenching, but the reverse effect is observed for dynamic quenching [34]. The quenching constants for the evaluation of the collisional quenching mechanism were analyzed by Stern-Volmer equation [34]:

$$F_0/F = 1 + K_{SV}[Q] = 1 + K_q \tau_0 [Q] \quad (1)$$

$$K_q = K_{SV} / \tau_0 \quad (2)$$

where F_0 and F are the fluorescence intensities in the absence and presence of quencher respectively. K_{SV} is the Stern-Volmer constant, and [Q] is the concentration of quencher (metronidazole). K_q is the bimolecular reaction rate constant, τ_0 (10^{-8} s) [33] is the average lifetime of biomolecule without quencher.

The quantitative analysis of the binding of metronidazole to ALDH was carried out using the fluorescence quenching at 350 nm at various concentrations, pH and temperatures. The regression curve of Stern-Volmer plots of the quenching of ALDH fluorescence by metronidazole at 25 °C is shown in Fig. 3. The plot was linear (R^2>0.94) at low concentration of the drug suggesting compliance with Stern-Volmer equation and curves upward as the concentration of the drug increases above 50 μM (a concentration ratio of 200 drug/enzyme). The Stern-Volmer constants were derived from Stern-Volmer obeys linearity. Table 1 summarizes the calculated the Stern-Volmer quenching constants (K_{SV} and K_q) at each temperature and pH studied. The results showed that the values of Stern-Volmer quenching constants K_{SV} increases with increasing temperature at all temperature. This suggested that the quenching mechanism of ALDH by metronidazole was dynamic quenching mechanism. At high concentrations it can be seen the deviation from linearity of the plots, suggesting that there are both types of quenching: static and dynamic quenching [34, 35]. This is not unusual. The study of BSA-metronidazole interaction [30, 31] presented the same

quenching pattern. However, pH change either to 5.0 or 9.0 did not alter this quenching pattern. The calculated apparent bimolecular quenching constant, K_q, were of the order of 10^{12} $L \cdot M^{-1} \cdot s^{-1}$ based on Eq. (1 and 2). The values were 100 times greater than the maximum permissible value for dynamic quenching i.e. 2×10^{10} $M^{-1} \cdot s^{-1}$. The result confirmed that the probable quenching mechanism of ALDH by metronidazole is a dynamic collision process.

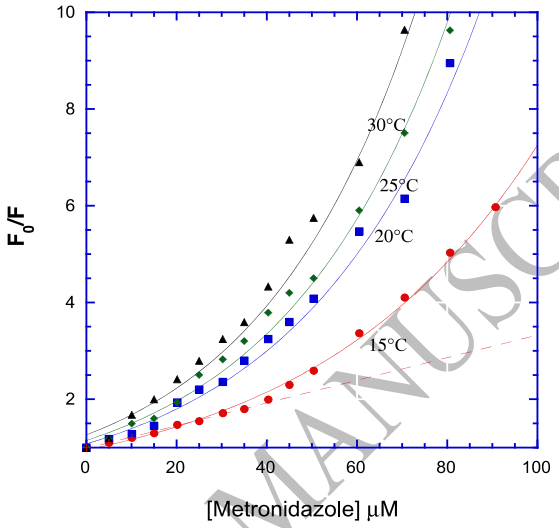

Fig. 3. The Stern-Volmer plots for the quenching of ALDH by metronidazole at different temperatures and pH = 7.4.

Table 1

Stern-Volmer quenching constants (K_{SV}) and bimolecular reaction rate constants (K_q) for the ALDH-metronidazole system at different temperatures and ph

	pH 5.0		**pH 7.4**		**pH 9.0**	
Temp. K	$K_{SV} \cdot 10^{-3}$ $L \cdot M^{-1}$	$K_q \cdot 10^{-11}$ $L \cdot M^{-1} \cdot s^{-1}$	$K_{SV} \cdot 10^{-3}$ $L \cdot M^{-1}$	$K_q \cdot 10^{-11}$ $L \cdot M^{-1} \cdot s^{-1}$	$K_{SV} \cdot 10^{-3}$ $L \cdot M^{-1}$	$K_q \cdot 10^{-11}$ $L \cdot M^{-1} \cdot s^{-1}$
288	6.5	6.5	5.7	5.7	5.5	5.5
293	7.9	7.9	8.0	8.0	7.7	7.7
298	8.2	8.2	8.5	8.5	7.9	7.9
303	9.2	9.4	8.9	8.9	8.2	8.2
308	9.4	9.7	9.6	9.6	8.5	8.5
313	9.7	9.8	9.9	9.9	9.8	9.8

BINDING CONSTANT AND NUMBER OF BINDING SITES

Quenching of intrinsic fluorescence was further used to assess the binding parameters [37]. The binding constant or affinity constant (K_a) of the metronidazole on the protein (ALDH) and number of binding sites (n) were calculated using the following equation, the Scatchard equation (modified Stern-Volmer plot):

$$\log\left(\frac{F_0 - F}{F}\right) = log\, K_a + n \cdot \log[Q] \quad (3)$$

The linear regression plot is shown in Fig. 4. Here, K_a and n were obtained from the slope and the intercept, respectively (Fig. 4.). The binding constant at all three pH (5.0, 7.4, and 9.0) were calculated. ALDH shows two binding sites for the drug (Table 2). The binding constant, K_a, between metronidazole and ALDH was of the order of 10^3 $L \cdot M^{-1}$, representing a moderate ligand-protein interaction. This is lower compared to BSA-metronidazole complex and one available binding site on human serum albumin for metronidazole as stressed earlier [30, 31]. Importantly, here, it was found that the value of K_a increases as the temperature increased. This coincided with the changes in the K_{SV}, and suggested that a dynamic quenching mechanism may explain the behaviour of the metronidazole-ALDH interactions.

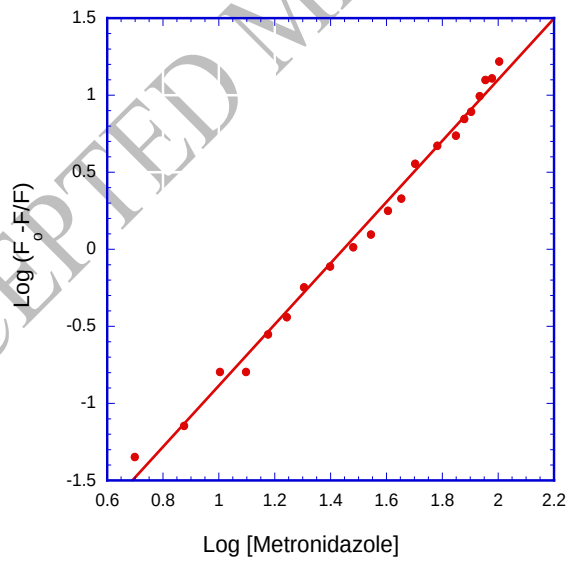

Fig. 4. Scatchard plot for the interaction between metronidazole and ALDH. [ALDH] = 0.250 μM, λ = 280 nm, pH = 7.4 in phosphate buffer 25 mM.

As a result, the metronidazole-ALDH linkage has an affinity of moderate strength and two binding sites for the drug (2 moles metronidazole to 1 mole ALDH) compared to metronidazole-HSA linkage which has higher affinity but of lower capacity. This might readily explains reported metronidazole intoxication in eukaryotic cell.

THERMODYNAMIC PARAMETERS AND NATURE OF INTERACTION FORCES

The interaction force between the ligand (i.e. drug) and biological macromolecule produce rarely covalent bond but usually hydrogen bond, van der Waals force, electrostatic force, or hydrophobic bonding [33]. The thermodynamic parameters are given by the enthalpy change (ΔH), entropy change (ΔS), and free energy change (ΔG) and they are used to predict the binding mode. The K_a dependence against temperature in the range of 288–313 K was evaluated by van't Hoff equation [34]:

$$\ln K_a = -\frac{\Delta H}{RT} + \frac{\Delta S}{R} \tag{4}$$

$$\Delta G = \Delta H - T\Delta S = -RT\ln K_a \tag{5}$$

The regression curve of ln K_a versus $1/T$ was linear as shown in Fig. 5 and produced negative values for ΔH (–33.30 kJ·M^{-1}) and ΔS (–171.04 J·M−1·K−1) at pH = 7.4. The positive ΔG values, 16.81 kJ·M^{-1} was obtained from eq. (5). The positive value of ΔG means that the binding process was non-spontaneous but however exothermic (ΔH<0) (Table 3). The enthalpic contribution was too low thus ruling out the possibility as metronidazole to forming covalent bonding with ALDH. The signs and magnitude of thermodynamic parameters, enthalpy variation (ΔH) and entropy variation (ΔS) for protein reactions are the main evidence for confirming the binding force [36]. The negative values of enthalpy variation ΔH and entropy variation ΔS suggest that the binding is mainly by van der Waals interaction and hydrogen bonding interaction. These interactions might be connected to ALDH polarity and its molecular configuration. pH change tends to alter the ionization of the ligand functional groups, the polarity of the solvent environment and conformation of enzyme and hence could affect the association constant of ligand binding [27]. This could consequently affect the energetics of binding. The influence of acidic pH (5.0) close from metronidazole pKa of 2.38 [45] and alkaline pH (9.0) at pI (near the isoelectric point of ALDH) on the interaction between metronidazole and ALDH was investigated. The summary of the result is shown in Table 2. The stoichiometry of the binding was not altered. The binding was non-spontaneous at both pH and is essentially based on van der Waals forces and maybe on hydrogen bond. The hydrogen bond is stronger than

a van der Waals interaction, but weaker than covalent or ionic bonds. However, the feasibility of the reaction was improved at pH closed to the pKa of metronidazole and ALDH optimum pH compared to other pHs of 7.4 and 5.0. Averagely, Δ*G* values at pH 9.0 was more feasible compared to pH 5.0 and pH 7.4. From this, it showed metronidazole pKa and ALDH optimum pH dictates the

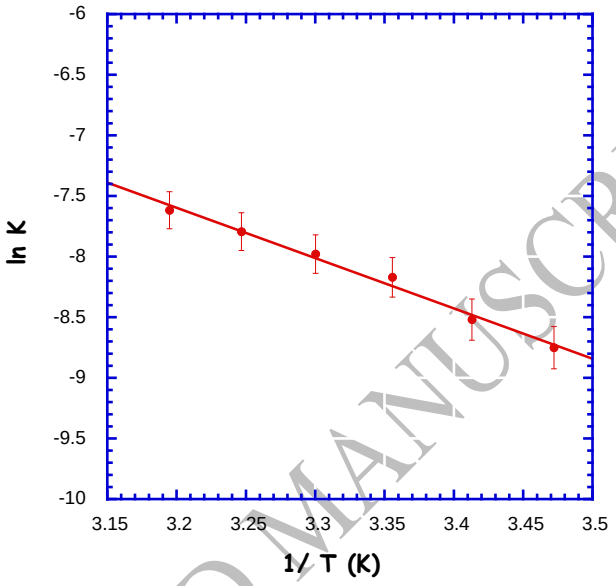

Fig. 5. Van't Hoff plot for the interaction between ALDH and metronidazole at pH = 7.4.

Table 2

The temperature and pH dependence of the number of binding site (*n*) and thermodynamic parameters of the metronidazole-ALDH system

Temp	**pH 5.0**				**pH 7.4**				**pH 9.0**			
K	*n*	Δ*H* kJ·M^{-1}	Δ*G* kJ·M^{-1}	Δ*S* J·M^{-1}·K^{-1}	*n*	Δ*H* kJ·M^{-1}	Δ*G* kJ·M^{-1}	Δ*S* J·M^{-1}·K^{-1}	*n*	Δ*H* kJ·M^{-1}	Δ*G* kJ·M^{-1}	Δ*S* J·M^{-1}·K^{-1}
288	1.5		16.82		1.5		15.96		1.9		16.91	
293	1.8		17.62		1.8		16.82		1.7		17.55	
298	1.6	–29.46	18.43	–160.68	1.8	–33.30	17.67	–171.04	1.7	–20.03	18.20	–128.27
303	1.5		19.23		1.5		18.53		1.8		18.84	
308	1.3		20.03		1.7		19.38		2.2		19.48	
313	1.6		20.84		1.9		20.24		1.6		20.12	

spontaneity of the reaction. The pHs stabilize the folded native structure of ALDH, while this does not interfere with the functionality of ALDH. In summary, ALDH must acquire a unique conformation in order to operate effectively. This is also crucial for its catalysis.

ALDH-METRONIDAZOLE DISSOCIATION

Protein-ligand interaction is a reversible interaction [45]. The reversibility is a function of association constant (K_a), dissociation constant K_d and binding free energy (ΔG). The net balance between K_a and K_d dictates the possible ligands/drugs transportation, therapeutic and or toxicity [45]. ALDH-metronidazole was treated as enzyme-inhibitor (EI) complex using previous assumptions [5, 36]. The dissociation constant, K_d was calculated as described elsewhere [5, 24].

$$\Delta F = \frac{\Delta F_{max}[L]}{K_d + [L]} \tag{6}$$

This was linearized to:

$$[L]/\Delta F = (K_d/\Delta F_{max}) + ([L]/\Delta F_{max}) \tag{7}$$

where ΔF_{max} is the maximum decrease in fluorescence observed when the enzyme is saturated by metronidazole. The validity of equation (7) is confirmed by the linearity of the Hanes-Woolf plot ($[L]/\Delta F$ vs. $[L]$). The result is presented in Fig. 6. The Hanes-Woolf plot for metronidazole concentration range (0 ÷ 105 μM) gave a K_d of 82.16 μM at pH 7.4 and 25 °C. The pattern of linearity and the statistical value of standard deviation (S.D.) of the K_d [40] clearly showed that metronidazole has one dissociation pattern to ALDH and exhibited a distinct K_d value within the concentration range. This confirmed that metronidazole has a dissociation mode with ALDH. The K_d value at other temperatures and pHs were also estimated. The K_d value strongly depends on the pH and temperature in the range we examined. The thermodynamics of dissociation constant was calculated from van't Hoff equation (equations (4) and (5)). The result is shown in Table 3. This clearly indicates that ionization of metronidazole dictates the dissociation of metronidazole-ALDH complex. As shown, the dissociation was very feasible at pH 5.0.

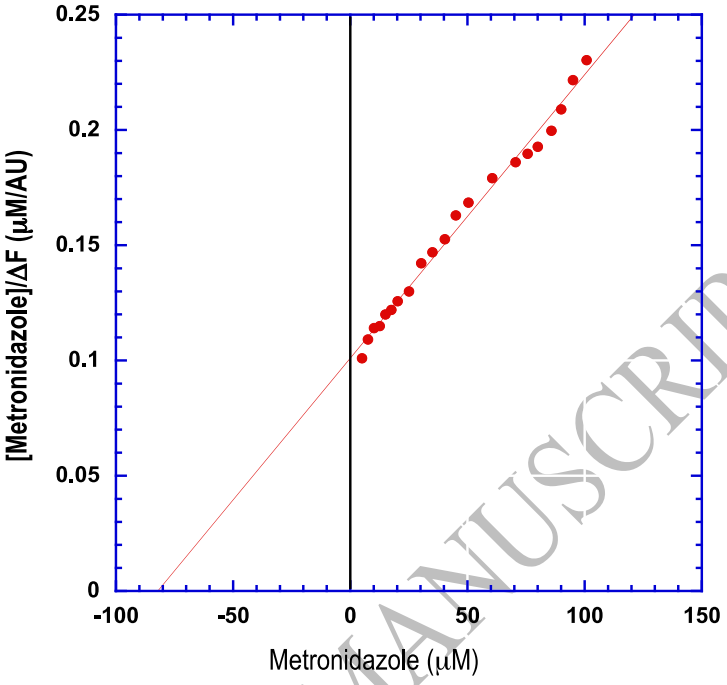

Fig. 6. The Hanes-Woolf plot of the quenching of the ALDH fluorescence in the presence of metronidazole at pH 7.4 and 25 ºC. The *x*-intercept of the linear regression represents $-K_d$ value in this study.

Table 3

The temperature dependence of thermodynamic parameters of the metronidazole-ALDH system between 15 ºC – 40 ºC, pH 5, 7.4, and 9 by van't Hoff plot

pH	5			7.4			9		
Temp K	ΔG_d kJ·M^{-1}	ΔH_d kJ·M^{-1}	ΔS_d J·M^{-1}	ΔG_d kJ·M^{-1}	ΔH_d kJ·M^{-1}	ΔS_d J·M^{-1}	ΔG_d kJ·M^{-1}	ΔH_d kJ·M^{-1}	ΔS_d J·M^{-1}
288	17.58			49.36			34.15		
293	19.02			56.75			29.74		
298	20.78	27.90	–120.38	59.84	27.32	–106.33	26.56	–13.65	–100.98
303	23.63			56.73			22.78		
308	25.14			52.67			19.54		
313	26.95			49.86			18.76		

Keys: ΔH = enthalpy change, ΔG = Gibb's free energy change, ΔS = entropy change, *d* index significates dissociation.

SYNCHRONOUS FLUORESCENCE SPECTRA AND UV-VISIBLE SPECTRA

Synchronous fluorescence spectroscopy provides information about the micro-environmental changes around protein intrinsic fluorophore functional groups [7]. The synchronous fluorescence spectra of ALDH were measured for Try residues and Trp residues when the wavelength interval $\Delta\lambda$ ($\Delta\lambda = \lambda em - \lambda ex$) is fixed at 15 and 60 nm, respectively [46]. Blue shift and red shift in $\lambda_{em\ max}$ signify the enhancement in hydrophobicity and polarity of the environment around the fluorophores (Tyr and Trp), respectively [29]. The results are shown in Fig. 7.a and b. The red shift of the position of the maximum wavelength indicates that the microenvironment of ALDH system was affected by metronidazole. The polarity around the tryptophan residues was increased and might likely increase the hydrodynamic volume of the ALDH. This exaggerated the results deduced from Fig. 2. The hydrophobicity of ALDH tryptophan residues was obvious based on the maximum emission wavelength (λ_{max}) and was more sensitive to change while the microenvironment around the tyrosine residues has less discernable change during the binding process. It was apparent that the fluorescence of tyrosine residues was weak. With this, we reckoned that metronidazole would bind a hydrophobic cavity within the vicinity of ALDH tryptophan residue and consequently affect the conformation of ALDHUV-Vis absorption spectroscopy was used to further explore the protein structural changes in the interaction of metronidazole with ALDH. The UV-Vis absorption spectra of ALDH in the absence and presence of metronidazole are shown in Fig. 8. The complex formed between metronidazole and ALDH was evident from the data of UV-Vis absorption spectra. ALDH has two absorption peaks, the absorption peak at 210 nm shows the conformation of the peptide bonds, while the peak of 272 nm are connected to aromatic amino acids [44]. The absorption maximum position of the metronidazole-ALDH was clearly visible. The red shift could indicate that metronidazole changes the peptide strands of the ALDH, the skeleton of ALDH becames loosen and the hydrophobicity decreases [12]. The absorption peak at about 278 nm can provide us information about the three buried aromatic amino acids: tryptophan, tyrosine, and phenylalanine. When the concentration of metronidazole increases, the ALDH molecules gradually become less compact. This might affect the activity of the enzyme.

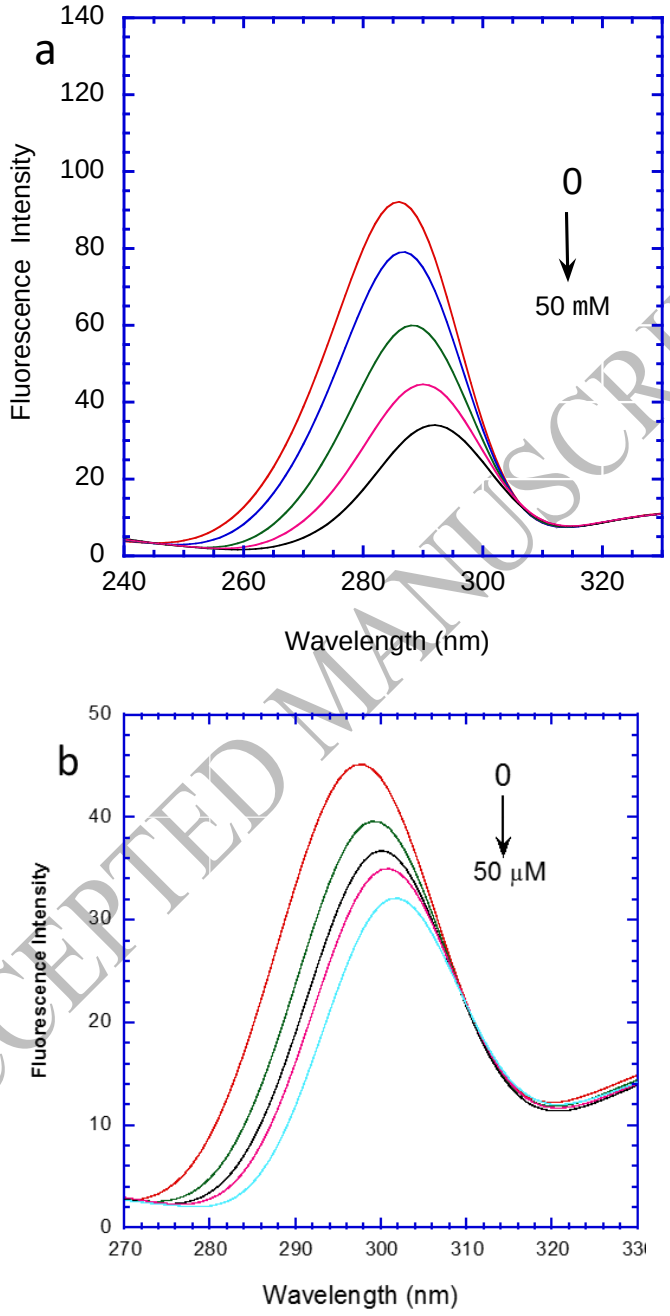

Fig. 7. Synchronous fluorescence spectra of ALDH in the presence of different concentrations of metronidazole: (a) Δλ = 60 nm (b) Δλ = 15 nm. Both at pH = 7.4; T= 25 °C.

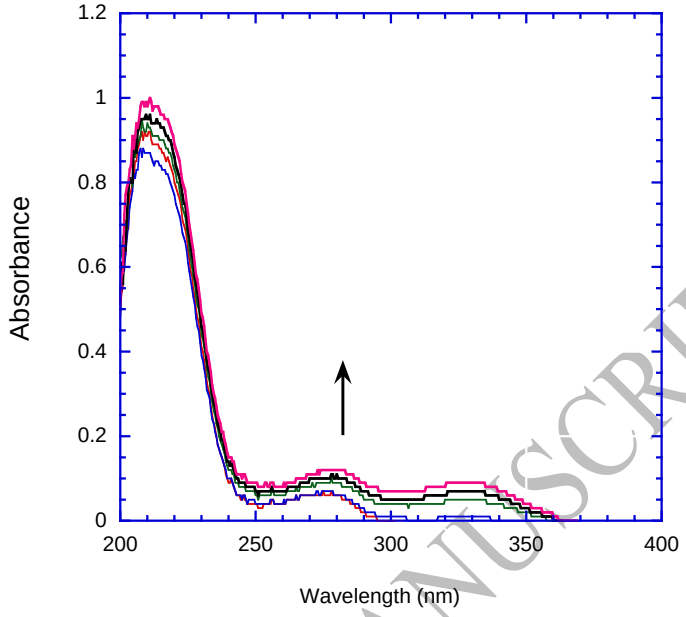

Fig. 8. The influence of metronidazole on UV-Visible absorption spectrum of ALDH. Spectra were obtained at pH = 7.4 and at temperature of 25 °C.

ENERGY TRANSFER FROM ALDH TO METRONIDAZOLE

As shown in Fig. 9, there is an obvious overlap between absorption spectrum of metronidazole (acceptor) and fluorescence spectrum of ALDH (donor) which forms the basis of fluorescence resonance energy transfer (FRET). According to Förster's non-radiative energy transfer theory [8], the energy transfer will likely happen when the donor can produce fluorescence light, fluorescence emission spectrum of the donor and UV absorption spectrum of the acceptor have more overlap and the distance between the donor (ALDH) and the acceptor (metronidazole) is lower than 8 nm [8, 17, 38]. The fluorescence quenching of ALDH upon binding with metronidazole indicated the energy transfer between metronidazole and ALDH. The efficiency of energy transfer, *E*, was calculated using the equation:

$$E = 1 - \frac{F_0}{F} = \frac{R_0^6}{R_0^6 + r^6} \tag{8}$$

where F and F_0 are the fluorescence intensities of ALDH in presence and absence of metronidazole, r the distance between acceptor and donor and R_0 the critical

distance when the transfer efficiency is 50%. The value of R_0 is calculated using the equation

$$R_0^6 = 8.79 \times 10^{25} K^2 \phi n^{-4} J \quad (9)$$

where K^2 is the spatial orientation factor of the dipole related to the random distribution of the donor and the acceptor; n is the refractive index of the medium; ϕ is the fluorescence quantum yield of the donor in the absence of acceptor and J is the spectral overlap integral between the fluorescence emission spectra of the donor and the absorption spectra of the acceptor, which can be calculated by the equation:

$$J = \sum F(\lambda) \cdot \varepsilon(\lambda) \cdot \lambda^4 \cdot \Delta\lambda / F(\lambda) \cdot \Delta\lambda \quad (10)$$

where $F(\lambda)$ is the donor fluorescence intensity at the wavelength of λ, and $\varepsilon(\lambda)$ is the molar absorption coefficient of the acceptor at the wavelength of λ. In the above equations, $K^2 = 2/3$, $n = 1.336$ and $\phi = 0.15$ [50]. From equations (8 - 10), J, R_0, E and r were calculated and are shown in Table 4. The binding distance was <7 nm and $0.5\ R_0 < r < 2.0\ R_0$. The results show that the non-radiative energy transfer occurs between metronidazole and ALDH.

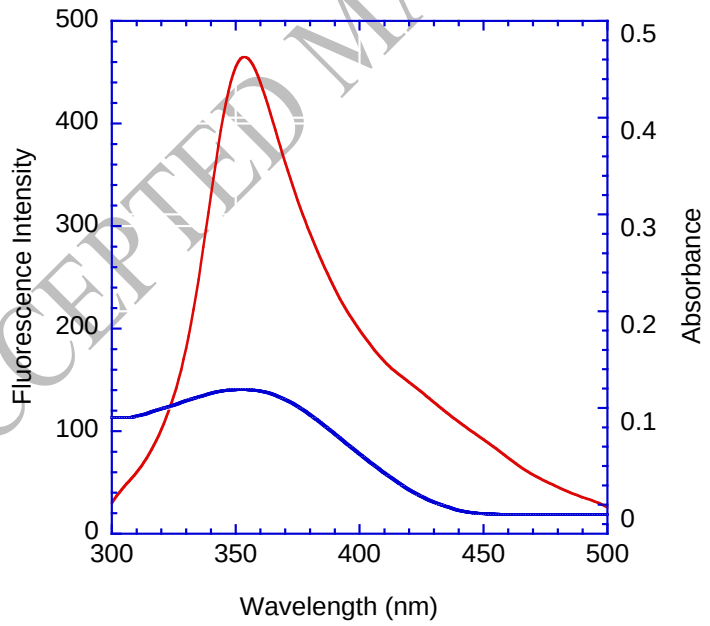

Fig. 9. The overlap of the fluorescence emission spectrum of ALDH (the upper curve, λ_{ex} = 280 nm, λ_{em} = 300–500 nm) with the absorption spectrum of metronidazole (the lower curve). T = 298 K; pH = 7.4.

Table 4

FRET data obtained from the overlapping of spectra of ALDH fluorescence emission and metronidazole absorption at 25 °C and pH = 7.4

J ($cm^3 \cdot L \cdot M^{-1}$)	R_o (nm)	r (nm)
1.682×10^{-14}	3.83	3.42

CONCLUSION

The present work provides an approach for studying the interactions of ALDH with metronidazole using absorption, fluorescence, and synchronous fluorescence techniques under physiological conditions. The results showed that ALDH fluorescence was quenched by metronidazole through dynamic quenching mechanism. Metronidazole interacted with ALDH through van der Waals forces and possible through hydrogen bonds. The distance between ALDH and bound metronidazole, based on FRET, is less than 8 nm; the secondary and tertiary structures of ALDH were altered. ALDH as nano-particles in a drug delivery of metronidazole prior to detoxification/intoxication is hereby suggested.

REFERENCES

1. BURTIN, P., A. TADDIO, O. ARIBURNU, T.R. EINARSON, G. KOREN, Safety of metronidazole in pregnancy, a meta-analysis, *Am. J. Obstet. Gynecol.*, 1995, **172**, 525–529.
2. CANPOLAT, E., M. KAYA, Synthesis and characterization of a new 5-bromosalicyliden-paminoacetophenone oxime and its complexes with Co(II), Ni(II), Cu(II) and Zn(II), *J. Coordination Chem.*, 2004, **57**, 12–17.
3. CHEN, J., X.Y. JIANG, X.Q. CHEN, Y. CHEN, Effect of temperature on the metronidazole-BSA interaction: multi-spectroscopic method, *J. Mol. Struct.*, 2017, **876**(1–3), 121–126.
4. CRABB, D. W., M. MATSUMOTO, D. CHANG, M. YOU, Overview of the role of alcohol dehydrogenase and aldehyde dehydrogenase and their variants in the genesis of alcohol-related pathology, *Proc. Nutr. Soc*., 2004, **63**(1), 49–63.
5. DABA, T., K. KOJIMA, K. INOUYE, Interaction of wheat β-amylase with maltose and glucose as examined by fluorescence, *J. Biochem.*, 2013, **154**(1), 85–92.
6. ESTEY, T., Y. CHEN, J.F. CARPENTER, V. VASILIOU, Structural and functional modifications of corneal crystallin ALDH3A1 by UVB ligh, *PLoS ONE*, 2010, **5**(12), 15218.
7. FAN, Y.C., S.L. ZHANG, J.C. KONG, Study on the interaction between anionic liquid and L-tryptophan by fluorescence spectroscopic technique, *J. Microchem*., 2011, **99**(2), 439–442.
8. FORSTER, T., Delocalized excitation and excitation transfer, in *Modern Quantum Chemistry*, O. Sinanoglu ed., Academic Press, New York, 1965, pp. 93–137.
9. FRAIJI, L.K., D.M. HAYES, T. WERNER, Static and dynamic fluorescence quenching experiments for the physical chemistry laboratory, *J. Chem. Ed.*, 1992, **69**, 424.
10. GRUNBLATT, E., P. RIEDERER, Aldehyde dehydrogenase (ALDH) in Alzheimer's and Parkinson's disease, *J. Neural. Transm.* (Vienna), 2016, **123**, 83–90.

11. HA, C.E., N.V. BHAGAVAN, Novel insights into the pleiotropic effects of human serum albumin in health and disease, *Biochim. Biophys. Acta*, 2013, **1830**, 5486–5493.
12. HU, Y.J., Y. LIU, J.B. WANG, X.H. XIAO, S.S. QU, Study of the interaction between monoammonium glycyrrhizinate and bovine serum albumin, *J. Pharm. Biomed. Anal.*, 2004, **36**, 915–919.
13. HU, Y., L. DA, Insights into the selective binding and toxic mechanism of microcystin to catalase, *Spectrochim. Acta Part A: Mol. Biomol. Spectroscopy*, 2014, **121**, 230–237.
14. KANDAGAL, P.B., S. ASHOKA, J. SEETHARAMAPPA, S.M.T. SHAIKH, Y. JADEGOUD, O.B. IJARE, Study of the interaction of an anticancer drug with human and bovine serum albumin: spectroscopic approach, *J. Pharm. Biomed. Anal.*, 2006, **41**, 393–399.
15. KELLER, M.A., U. ZANDER, J.E. FUCHS, C. KREUTZ, K. WATSCHINGER, T. MUELLER, G. GOLDERER, K.R. LIEDL, M. RALSER, B. KRÄUTLER, E.R. WERNER, J.A. MARQUEZ, 2A gatekeeper helix determines the substrate specificity of Sjogren-Larsson Syndrome enzyme fatty aldehyde dehydrogenase, *Nature. Comm.*, 2014, **5**, 4439.
16. KOPPAKA, V., D.C. THOMPSON, Y. CHEN, M. ELLERMANN, K.C. NICOLAOU, R.O. JUVONEN, Aldehyde dehydrogenase inhibitors: a comprehensive review of the pharmacology, mechanism of action, substrate specificity, and clinical application, *Pharmacol. Rev.*, 2012, **64**, 520–539.
17. LAKOWICZ, J.R., *Principles of Fluorescence Spectroscopy*, 3rd ed., Springer, New York, 2006.
18. LEE, H.S., T. ISSE, T. KAWAMBOTO, H.W. BAIK, J.Y. PARK, M. YANG, Effect of Korean pear (*Pyruspyrifolia* cv. Shingo) juice on hangover severity following alcohol consumption, *Food Chem. Toxicol.*, 2013, **58**, 101–106.
19. MA, I., A.L. ALLAN, The role of human aldehyde dehydrogenase in normal and cancer stem cells, Stem Cell Rev., 2011, **7(2)**, 292–306.
20. MACGIBBON, A.K.H., L.F. BLACKWELL, P.D. BUCKLEY, Kinetics of sheep-liver cytoplasmic aldehyde dehydrogenase, *Eur. J. Biochem.*, 1977, **77**, 93–100.
21. MACGIBBON, A.K.H., P.D. BUCKLEY, L.F. BLACKWELL, Evidence for two-step binding of reduced nicotinamide adenine dinucleotide to aldehyde dehydrogenase, *Biochem. J.*, 1977, **165**, 455–462.
22. MAHFOUZ, N.M., M.A. HASSAN, Synthesis, chemical and enzymatic hydrolysis, and bioavailability evaluation in rabbits of metronidazole amino acid ester prodrugs with enhanced water solubility, *J. Pharm. Pharmacol.*, 2001, **53**(6), 841–848.
23. MUZIO, G., M. MAGGIORA, E. PAIUZZI, M. ORALDI, R.A. CANUTO, Aldehyde dehydrogenases and cell proliferation, *Free Radical Biol. Med.*, 2012, **52**, 735–746.
24. OHNISHI, M., T. YAMASHITA, K. HIROMI, Static and kinetic studies by fluorometry on the interaction between gluconolactone and glucoamylase from *Rh. niveus*, *J. Biochem.*, 1977, **8**, 99–105.
25. PAN, X., P. QIN, R. LIU, J. WANG, Characterizing the interaction between tartrazine and two serum albumins by a hybrid spectroscopic approach, *J. Agric. Food Chem.*, 2011, **59**, 6650–6656.
26. PAPPA, A., T. ESTEY, R. MANZER, D. BROWN, V. VASILIOU, Human aldehyde dehydrogenase 3A1 (ALDH3A1): Biochemical characterization and immunohistochemical localization in the cornea, *Biochem. J*., 2003, **376**(3), 615–623.
27. PARAJULI, B., M.L. FISHEL, D.T. HURLEY, Selective ALDH3A1 inhibition by benzimidazole analogues increase mafosfamide sensitivity in cancer cells, *J. Med. Chem*., 2014, **57**, 449–461.
28. PETERS T., All about Albumin: Biochemistry, Genetics and Medical Application, Academic Press, San DIEGO, CA, USA., 1996.
29. RAHNAMA, E., M. MAHMOODIAN-MOGHADDAM, S. KHORSAND-AHMADI, M.R. SABERI, J. CHAMANI, Binding site identification of metformin to human serum albumin and

glycated human serum albumin by spectroscopic and molecular modeling techniques: a comparison study, *J. Biomolec. Struct. Dynamics*, 2015, **33**, 513–533.
30. ROSENKRANZ, H. S., W.T. PECK, Mutagenicity of metronidazole: Activation by mammalian liver microsomes, *Biochem. Biophys. Res. Comm.*, 1975, **66**(2), 520–525.
31. ROSS, P. D., S. SUBRAMANIAN, Thermodynamics of protein association reactions: forces contributing to stability, *Biochemistry*, 1981, **20**, 3096–3102.
32. RUTGEERTZ, P., M. HIELE, K. GEBOES, M. PEETERS, F. PENNINCKS, R. AERTS, R. KERREMANS, Controlled Trial of Metronidazole Treatment for prevention of Crohn's recurrence after ileal resection, *Gastroenterology*, 2015, **108**(6), 1617–1621.
33. SIDDIQI, M.K., P. ALAM, S.K. CHATURVEDI, R.H. KHAN, Anti-amyloidogenic behavior and interaction of diallylsulfide with human serum albumin, *Int. J. Biol. Macromol*., 2016, **92**, 1220–1228.
34. SONG, H., C. CHEN, S. ZHAO, F. GE, D. LIU, D. SHI, T. ZHANG, Interaction of gallic acid with trypsin analyzed by spectroscopy, *J. Food Drug Analysis*, 2015, **23**, 234–242.
35. STEINMETZ, C.G., P. XIE, H. WEINER, T.D. HURLEY, Structure of mitochondrial aldehyde dehydrogenase: the genetic component of ethanol aversion. *Structure*, 1997, **5**, 5701–5711.
36. TANAKA, T., T. KOJIMA, T. KAWAMORI, A. WANG, M. SUZUI, K. OKAMOTO, H. MORI, Inhibition of 4-nitroquinoline-1-oxide-induced rat tongue carcinogenesis by the naturally occurring phenolic caffeic, ellagic, chlorogenic and ferulic acids, *Carcinogenesis*, 1993, **14**, 1321–1325.
37. TOPRAK, M., Fluorescence study on the interaction of human serum albumin with Butein in liposomes, *Spectrochim. Acta Part A: Mol. Biomol. Spectroscopy*, 2016, **154**, 108–113.
38. VALEUR, B., J.C. BROCHON, *New Trends in Fluorescence Spectroscopy*, Springer, Berlin, 1999.
39. VAN DE WEERT, M., Fluorescence quenching to study protein-ligand binding: common errors, *J. Fluoresc*., 2010, **20**, 625‒629.
40. WROCZYNSKI, P., J. WIERZCHOWSKI, Aromatic aldehydes as fluorogenic indicators for human aldehyde dehydrogenases and oxidases: substrate and isozyme specificity, *Analyst*, 2000, **125**, 511–516.
41. WU, Y., R. FASSINI, Stability of metronidazole, tetracycline HCl and famotidine alone and in combination, *Int. J. Pharmacol*., 2005, **290**, 1–13.
42. WYMORE, T., J. HEMPEL, S.S. CHO, A.D. MACKERELL JR., H.B. NICHOLAS JR., D.W. DEERFIELD, Molecular recognition of aldehydes by aldehyde dehydrogenase and mechanism of nucleophile activation, *Proteins*, 2004, **57**(4), 758–771.
43. XIAO-YAN, L., Interaction of metronidazole with bovine serum albumin by using fluorescence and resonance light scattering spectra, *Acta Phys. Chim. Sin*., 2007, **23**(2), 262–267.
44. ZHANG, Y.Z., X.X. CHEN, J. DAI, X.P. ZHANG, Y.X. LIU, Y. LIU, Spectroscopic studies on the interaction of lanthanum (III) 2-oxo-propionic acid salicyloyl hydrazone complex with bovine serum albumin, *Luminescence*, 2008, **23**, 150–156.
45. ZHOU, C., Y. JIN, J.R. KENSETH, M. STELLA, K.R. WEHMEYER, W.R. HEINEMAN, Rapid pK_a estimation using vacuum-assisted multiplexed capillary electrophoresis (VAMCE) with ultraviolet detection, *J. Pharm. Sci*., 2005, **94**, 576–589.
46. ZHOU, N., Y.Z. LIANG, P. WANG, 18β-Glycyr-rhetinic acid interaction with bovine serum albumin, *Photochem. Photobiol. A: Chemistry*, 2007, **185**, 271–276.
47. ZHU, X.S., A.Q. GONG, B.S. WAN, Study on the interaction of tropisetr on hydrochloride and L-tryptophan by spectrofluorimetry and its analytical application, *J. Lumin.*, 2008, **128**(11), 1815–1818.
48. ZIYARAT, P. F., A. ASOODEH, Z.S. BARFEH, M. PIROUZI, J. CHAMANI, Probing the interaction of lysozyme with ciprofloxacin in the presence of different-sized Ag nano-particles by

multispectroscopic techniques and isothermal titration calorimetry, *J. Biomol. Struct. Dynamics*, 2014, **32**, 613–629.
49. ***5 drugs commonly abused by Nigerians and their adverse effects, https://www.nigerianbulletin.com/threads/5-drugs-commonly-abused-by-nigerians-and-their-adverse-effects.113260/.
50. ****IARC Monographs on the Evaluation of Carcinogenic Risks to Humans – Overall Evaluations of Carcinogenicity*, Supplement 7, Lyon, France, 1987.